



www.asianpubs.org

ARTICLE

## Quantum Computational, Spectroscopic, NBO and Molecular Docking Studies on 1-Methylnicotinamide (MNA): An Antithrombotic, Anti-inflammatory, Gastroprotective and Vasoprotective Compound

Mukesh Kumar<sup>1</sup>, Satyavir Singh<sup>1</sup>,  
Nazia Siddiqui<sup>2</sup> and Saleem Javed<sup>3,✉,iD</sup>

### ABSTRACT

In present work, 1-methylnicotinamide (1-MNA) has been investigated theoretically by density functional theory approach and investigated its vibrational spectroscopy. To complete the structure optimization, determination of vibrational frequencies and other valuable parameters, B3LYP method used with the 6-311++G(d,p) basis set. Atoms in molecules theory (AIM) had been used to evaluate ellipticity, isosurface projection by electron localization function and binding energies. The IR and Raman spectra have also been calculated computationally. NBO analysis employed to determine interactions of donor and acceptor. Fukui functions and molecular electrostatic potential (MEP) showed reactive regions of the molecule. UV-vis spectrum calculated using TD-DFT/PCM methods with different solvents. Thermodynamic properties like free energy, enthalpy and entropy with various temperature were calculated. By the use of the electrophilicity index, the probability of the bioactive nature of the molecule was proved theoretically. Protein-ligand interactions calculated and established by molecular docking. The biological investigations for druglikeness also employed for the (1-MNA).

### KEYWORDS

1-Methylnicotinamide, Density functional theory, Natural bond orbital, Molecular docking, Ellipticity, Molecular electrostatic potential.

### INTRODUCTION

An essential nutrient nicotinamide can be autogenously metabolized in the liver by enzyme nicotinamide *N*-methyltransferase (NNMT) to 1-methylnicotinamide (1-MNA). Earlier 1-MNA was supposed to be biologically inactive substance, however, recent studies show remarkable and tremendous therapeutic applications of this compound. Several biological studies on 1-MNA proves that it has antithrombotic [1,2], anti-inflammatory [3], gastroprotective and vasoprotective [4] properties. 1-Methylnicotinamide is also a signalling molecule formed in skeletal muscle to regulate energy metabolism [5] and can regulate trombolytic and inflammatory processes in the cardiovascular system [6]. Recent study showed that 1-MNA can extend life-span of diabetic rats [7]. Also, 1-MNA and its structural

## Asian Journal of Organic & Medicinal Chemistry

Volume: 6                      Year: 2021  
Issue: 2                        Month: April–June  
pp: 128–140  
DOI: <https://doi.org/10.14233/ajomc.2021.AJOMC-P326>

Received: 25 May 2021

Accepted: 23 June 2021

Published: 24 July 2021

#### Author affiliations:

<sup>1</sup>Department of Chemistry, Shri Khushal Das University, Hanumangarh-335801, India

<sup>2</sup>USIC, Dayal Bagh Educational Institute Agra-282005, India

<sup>3</sup>Department of Chemistry, I.H.S. Khandari, Dr. Bhimrao Ambedkar University, Agra-282002, India

✉To whom correspondence to be addressed:

E-mail: [saleem.7javed@gmail.com](mailto:saleem.7javed@gmail.com), [dr.naazsiddiqui@gmail.com](mailto:dr.naazsiddiqui@gmail.com)

Available online at: <http://ajomc.asianpubs.org>

analogs were found to prevent cancer metastasis [8]. Other than that 1-MNA can extend lifespan of diabetic rats, used in many cosmetic products like hair and skin care products and as a dietary supplement [9]. In spite of huge biological applicability, the 1-MNA has not been theoretically explored earlier by any research groups.

This study includes density functional theory (DFT) approach to study structural, vibrational along with spectroscopic details like UV-visible, Raman, IR. Analysis of non-linear optical properties, Frontier molecular orbital and molecular electrostatic potential (MEP) were also achieved. Scrutiny of results will provide better understanding for expected intermolecular interactions among the atoms of the studied molecule, which in turn assists the justification of drug-receptor intermolecular interactions and provide the path for scheming new nicotinamide bearing biologically active molecules.

### COMPUTATIONAL DETAIL

The density functional theory (DFT) is an adequate tool among various quantum methods to describe important properties of the molecule. For better representation of polar bonds, enhancement of the lower basis sets was carried out by applying 'd' and 'p' polarization functions for heavy and hydrogen atoms respectively. Majority of calculations were executed with B3LYP functional and 6-311++G(d,p) basis set [10,11] which are provided in the Gaussian 03W program package [12] and some of results are also obtained by ORCA (4.0.1) [13]. The optimized molecular structure is used to attain number of molecular properties such as, geometrical parameters, vibrational wavenumbers, HOMO-LUMO, natural bond orbitals (NBO) and molecular electrostatic potential (MEP). VEDA4 [14] software was used to assign vibrations along with their PED (potential energy distribution). Use of atoms in molecule (AIM) theory to determine electron localization function and electron density ellipticity were also done. Molecular docking was also carried out using Autodock-vina software. The SwissADME tool [15] provides drug-likeness character of molecule, which is important for any drug development. Multiwfn software [16] for visualization and Origin8.0 software [17] for plotting graphs were used.

### RESULTS AND DISCUSSION

**Optimized molecular geometry:** For complete structure optimization B3LYP method used with 6-311++G(d,p) basis set. The obtained bond length and bond angles after optimization are summarized in Table-1 in ESI. The optimized structure with labelled atoms is shown in Fig. 1. Since title compound is not symmetrical therefore, it has C1 point group. The calculated C-C-C and C-C-N bond angles for pyridine ring are ranges in between 119.29 -121°. While C-C-H bond angle in the ring ranges from 116.5-122.9°. The bond lengths of C-H almost remains same. The C-C ranges 1.38-1.40 Å because of ring nitrogen. The bond lengths of all C-H bonds are found almost similar (1.08 Å). The C1-N6 and C5-N6 bond lengths are same (1.35 Å) with experiment bond lengths but shorter than N6-C16, (1.48 Å). On the other hand the bond length of C11-O12 is shorter (1.21 Å) than any C-C or C-N bond as usual. The bond angle C2-C11-N13 (116.63°) also lesser than any ring

TABLE-1  
OPTIMIZED GEOMETRICAL PARAMETERS OF  
1-METHYLNICOTINAMIDE (1-NMA): BOND  
LENGTH (Å) AND BOND ANGLES (°)

Parameter	B3LYP/6-311++G(d,p)	Parameter	B3LYP/6-311++G(d,p)
Bond length (Å)		Bond angle (°)	
C1-C2	1.3837	C1-C2-C11	123.0829
C1-N6	1.3551	C3-C2-C11	118.0868
C1-H8	1.0820	C2-C3-C4	119.6572
C2-C3	1.3995	C2-C3-H7	118.8149
C2-C11	1.5199	C4-C3-H7	121.5248
C3-C4	1.3902	C3-C4-C5	119.2909
C3-H7	1.0838	C3-C4-H9	121.5027
C4-C5	1.3830	C5-C4-H9	119.2022
C4-H9	1.0821	C4-C5-N6	120.6398
C5-N6	1.3515	C4-C5-H10	122.859
C5-H10	1.0817	C6-C5-H10	116.499
N6-C16	1.4860	C1-N6-C5	120.7857
C11-O12	1.2115	C1-N6-C16	119.4931
C11-N13	1.3604	C5-N6-C16	119.6634
N13-H14	1.0082	C2-C11-O12	118.4319
N13-H15	1.0118	C2-C11-N13	116.6391
C16-H17	1.0877	O12-C11-N13	124.8768
C16-H18	1.0905	C11-N13-H14	122.0403
C16-H19	1.0876	C11-N13-H15	116.4398
Bond angle (°)		N6-C16-H17	109.1241
C2-C1-N6	120.9925	N6-C16-H18	109.1976
C2-C1-H8	122.9056	N6-C16-H19	109.0373
N6-C1-H8	116.0706	H17-C16-H18	110.0475
C1-C2-C3	118.602	H17-C16-H19	109.3931
		H18-C16-H19	110.0194

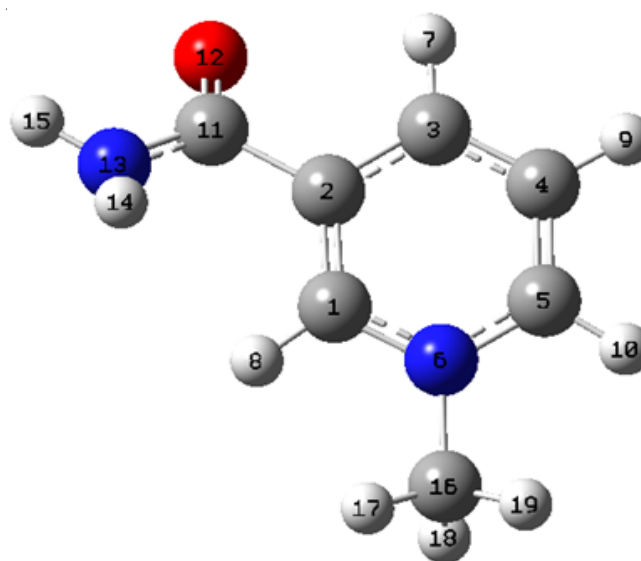


Fig. 1. Optimized structure of 1-methylnicotinamide (1-NMA) with atom numbering, blue coloured is nitrogen, brown coloured are carbon and red coloured is oxygen

angle of three atoms. The presence of nitrogen atom in the ring, makes the bond angles slightly distorted from the perfect hexagonal structure.

**Vibrational spectral analysis:** The simulation of IR and Raman spectrum of 1-MNA was done by using B3LYP-6-311++ G(d,p) basis set with scaling factor 0.961 (as reported for the similar compounds) [18]. There are no imaginary frequencies present in the calculated vibrational analysis

indicating that the optimized geometry is present at the lowest site on the potential energy surface.

1-Methylnicotinamide (MNA) has 19 atoms and 51 modes of vibrations and symmetry possess  $C_s$  and  $C_1$  point group. IR and Raman activity found for vibrations. The VEDA program

[14] facilitate to calculate the partial energy distribution (PED) and with the help of PED fundamental vibrational modes were characterized. Almost all fundamental modes of vibrations possess significant percentage of PED under  $C_1$  symmetry. Table-2 contains the calculated IR and Raman frequencies.

TABLE-2  
CALCULATED VIBRATIONAL FREQUENCIES ( $\text{cm}^{-1}$ ) ASSIGNMENTS OF  
1-METHYLNICOTINAMIDE (1-NMA) BASED ON B3LYP/6-311++G(d,p) BASIS SET

Mode No.	Theoretical wave number ( $\text{cm}^{-1}$ )		$I_{\text{IR}}^c$	$I_{\text{RAMAN}}^d$	Assignments (PED) <sup>a,b</sup>
	Unscaled	Scaled			
51	3686	3543	18	25	$\gamma_{\text{as}}$ NH(98)
50	3564	3426	31	84	$\gamma_{\text{s}}$ NH(98)
49	3227	3102	2	83	$\gamma$ CH(61)
48	3217	3094	2	8	$\gamma$ CH(29)
47	3216	3093	2	50	$\gamma$ CH(49)
46	3204	3080	2	24	$\gamma$ CH(46)
45	3175	3052	0	20	$\gamma$ CH(96)
44	3156	3034	0	30	$\gamma$ CH(94)
43	3071	2952	0	100	$\gamma$ CH(96)
42	1783	1714	100	21	$\gamma$ OC(77)
41	1661	1597	8	13	$\gamma$ CC(46) + $\beta$ HCC(15)
40	1631	1568	30	4	$\beta$ HCH(81)
39	1620	1557	3	7	$\beta$ HCC(13)
38	1531	1472	30	1	$\gamma$ CC(14) + $\beta$ HCC(26) + $\beta$ HCH(10)
37	1505	1447	6	1	$\beta$ HCC(15) + $\beta$ HCH(35) + $\tau$ HCNC(12)
36	1489	1432	5	5	$\beta$ HCH (58) + $\tau$ HCNC(24)
35	1474	1417	1	3	$\gamma$ CC(14) + $\beta$ HCH(25)
34	1451	1395	1	3	$\beta$ HCH(68)
33	1372	1318	63	12	$\gamma$ NC(19) + $\gamma$ CC(20) + $\beta$ ONC(14)
32	1355	1302	0	0	$\beta$ HCC(29)
31	1335	1283	0	1	$\gamma$ CC(34) + $\gamma$ NC(30) + $\tau$ HCNC(10)
30	1225	1178	8	1	$\gamma$ NC(29) + $\beta$ HCC(29)
29	1210	1163	5	5	$\gamma$ NC(15) + $\beta$ HCC(19) + $\beta$ CCN(16)
28	1162	1117	1	0	$\beta$ HCC(18) + $\tau$ HCNC(13)
27	1146	1102	2	0	$\beta$ HCH(14) + $\tau$ HCNC(38)
26	1144	1100	2	1	$\gamma$ CC(14) + $\beta$ HCC(13) + $\tau$ HCNC(17)
25	1095	1053	0	5	$\gamma$ OC(10) + $\gamma$ NC(12) $\tau$ + $\beta$ HNC(48)
24	1085	1043	2	0	$\gamma$ NC(13) + $\tau$ HCNC(28)
23	1046	1006	1	27	$\gamma$ CC(25) + $\beta$ CCC(20) + $\beta$ CCNC(13) + $\beta$ CNC(11)
22	1031	991	0	0	$\beta$ CCC(38) + $\tau$ CCNC(12)
21	979	941	0	0	$\tau$ CCNC(54)
20	933	896	2	0	$\tau$ HCCC(22)
19	895	860	2	0	$\gamma$ NC(28) + $\gamma$ CC(15) + $\beta$ CCN(12)
18	839	806	6	0	$\tau$ HCCC(51)
17	755	726	12	0	$\tau$ ONCC(65)
16	734	706	0	7	$\gamma$ NC(19) + $\beta$ CCN(28)
15	683	657	5	0	$\tau$ HCCC(26) + $\tau$ CCNC(36)
14	637	612	8	1	$\beta$ ONC(48)
13	593	570	18	0	$\tau$ HNCC(50)
12	550	529	2	1	$\gamma$ NC(11) + $\beta$ CCC(12) + $\beta$ CNC(27)
11	523	503	3	3	$\gamma$ NC(13) + $\beta$ CNC(28)
10	446	429	9	0	$\beta$ CNC(10) + $\tau$ HNCC(17) + $\tau$ CCNC(11) + $\tau$ CCCN(16)
9	420	404	21	0	$\tau$ HNCC(28) + $\tau$ CCNC(27)
8	391	376	12	0	$\beta$ CNC(13) + $\tau$ HNCC(22) + $\tau$ CCNC(17)
7	370	356	1	1	$\beta$ CNC(33)
6	352	337	2	1	$\gamma$ CC(30) + $\beta$ ONC(19) + $\beta$ CNC(14)
5	202	194	1	0	$\tau$ CCNC(10) + $\tau$ CNCC(26) + $\tau$ CCCN(46)
4	141	136	2	1	$\tau$ CCCC(38)
3	116	112	1	0	–
2	51	49	3	1	$\tau$ CNCC(49)
1	50	48	0	0	$\tau$ HCNC(79)

<sup>a</sup> $\gamma$ -stretching,  $\beta$ -bending,  $\tau$ -torsion; <sup>b</sup>Scaling factor: 0.961 for B3LYP/6-311++G(d,p); <sup>c</sup>Relative absorption intensities normalized with highest peak absorption equal to 100; <sup>d</sup>Relative Raman intensities normalized to 100.

Figs. 2 and 3 shows the simulated Raman and IR spectra of 1-methyl-nicotinamide (1-NMA).

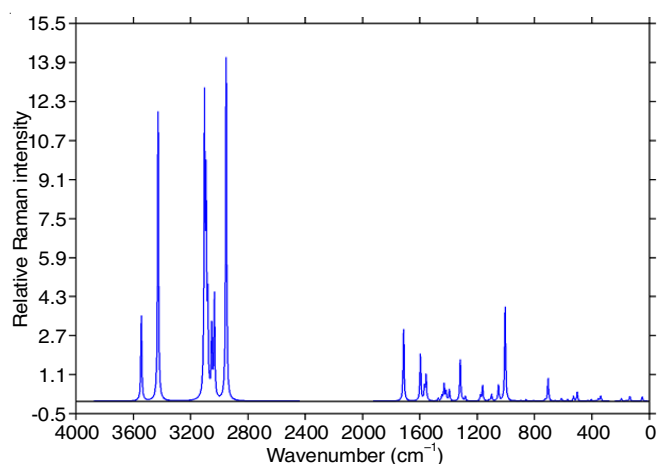


Fig. 2. Calculated Raman spectra of 1-methylnicotinamide (1-NMA) using DFT/6-311++G(d,p)

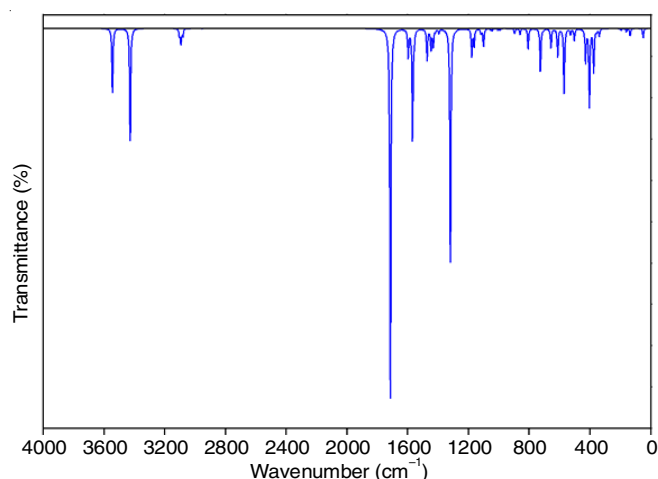


Fig. 3. Calculated computational infrared spectra of 1-methylnicotinamide (1-NMA) using DFT/6-311++G(d,p)

**N-H and C-O vibrations in amide group:** The N-H stretching vibrations for all heterocyclic compounds normally falls in the region 3500-3000  $\text{cm}^{-1}$  [19]. Since MNA has one  $\text{NH}_2$  in amide group therefore, it is expected by  $\text{NH}_2$  group to show one symmetric and one asymmetric mode of N-H vibration and it is also expected that the asymmetric stretching of NH (mode no. 51) will have higher magnitude than the symmetric stretching (mode no. 52) [15] these modes seem from 3543 to 3436  $\text{cm}^{-1}$  [20,21]. The PED of N-H mode is 98% with strong peaks. The C-O stretching frequency is 1714  $\text{cm}^{-1}$  with 77% PED shows most intense peak in IR spectrum. This stretching frequency of C-O is little higher side because of pyridine ring.

**C-H vibrations:** The characteristic region of C-H ring stretching vibrations is in the range of 3100-2950  $\text{cm}^{-1}$ . Therefore, it is confirmed by the presence of strong Raman intensity of C-H stretching vibration. Different substituents do not much influence the bands [22]. The title compound has four C-H bonds in pyridine ring and three C-H bonds in methyl group. The predicted four C-H stretching vibrations correspond to mode from 43 to 49 (Table-2) shows stretching modes of C1-H, C3-H, C4-H, C5-H and three C16-H bonds. The computed

C-H stretching vibrations frequencies are 3102, 3094, 3093, 3080 and 3052  $\text{cm}^{-1}$ .

**C-C vibrations:** Generally, the carbon vibrations of heterocyclic aromatic compounds found between 1400 and 1650  $\text{cm}^{-1}$  [23]. The actual positions do not determine by the substituents and the form [24]. The expected (C=C) ring stretching vibrations found in the region 1300-1000  $\text{cm}^{-1}$  [25]. The calculated C-C stretching vibrations were 1597, 1472, 1417, 1318, 1283, 1100 and 1006  $\text{cm}^{-1}$  and C-N stretching vibrations were 1318, 1178, 1163, 1043 and 860  $\text{cm}^{-1}$ . The observed PED analysis showed that the vibrations of given molecule is mixed modes given in Table-2. All the C-C, C=C and C-N bands are within the expected range.

Because of the presence of one N atom present in the ring small variation found in C=C stretching. The bending modes of C-C-C, C-C-N and C-N-O are assigned to the bands at 1006, 991, 806, 706, 529, 503, 429, 404 and 612  $\text{cm}^{-1}$ . These modes also shows mix modes in PED.

**C-N vibrations:** The assignment of C-N stretching band is a difficult task in the side chain due to mixing. C-N stretching frequency determined by Pinchas *et al.* [26] at 1368  $\text{cm}^{-1}$  in benzamide. The C=N showed peek at around 1500  $\text{cm}^{-1}$ , If C-N band appears close to 1300  $\text{cm}^{-1}$  then it suggest that C-N bonds are present [23]. Theoretically scaled values were found at 1318, 1283, 1178, 1163, 1053, 1043, 860 and 706  $\text{cm}^{-1}$ . The PED of these vibrations are present in Table-2.

**Molecular electrostatic potential (MEP) surface:** The molecular electrostatic potential surface indicates 3D charge distributions of molecules. If we can predict the charge distribution in the molecule, then it will be very useful to determine molecular interactions and the character of the bond. It is really important because electrostatic potential shows colour grading corresponds to many characteristic properties of the molecule like shape, size, positive negative and neutral charge. Therefore this idea is important to analyze different physicochemical properties of a molecule [27]. The colours distribution in Fig. 4 shows the different electrostatic potential at the surface of the given molecule.

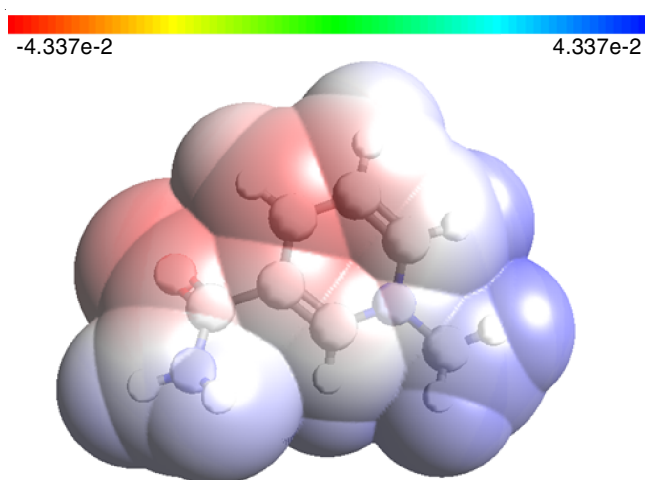


Fig. 4. Molecular electrostatic potential (MEP) of 1-methylnicotinamide (1-NMA)

The increasing order of electrostatic potential has been given as: red < orange < yellow < green < blue. The range of

the map is from  $-4.337e-2$  a.u. (deepest red) to  $4.337e-2$  a.u. (deepest blue). The strongest repulsion that is electrophilic attack is indicated by red colour while strongest attraction that is nucleophilic attack shows by blue colour.

The lone pair of electronegative atoms normally present with negative  $V(r)$  value. Fig. 4 shows presence of negative electrostatic potential on the ring nitrogen atom while hydrogen atoms associated with nitrogen showing positive electrostatic potential in the amide group. Hydrogens of methyl group is also showing positive electrostatic potential. The white colour indicates the neutral region present in between both the ends, red and blue [28]. The charge regions in the molecule will be important to know intermolecular interactions and MEP diagram also shows the behaviour to approaching protons.

**Electron localization function (ELF):** Electron localization function provides better understanding of localization of electrons as electron pairs present in the Lewis structures. ELF is the measure of excess kinetic energy density of Pauli repulsion. The ELF value near to 1 indicates the strong probability of finding paired or single electron and this value also shows maximum Pauling repulsion and 0 ELF value indicates minimum repulsion region. Therefore well localized electrons possess strongest Pauli repulsion which would present in chemical bonds, as lone pair electrons, *etc.* Thus ELF analysis is an important parameter to give information about molecular structure, chemical bonding and reactivity [29]. The ELF values may be shown by using 2D and 3D graphs with the help of colour coding and shaded contours shown in Fig. 5. Red colour indicates ELF values near to 1 while decreasing values given from yellow to green (about 0.7) and the least value near to 0 indicated by blue colour. The space near the hydrogen shows maximum Pauli repulsion and indicated with red colour region. While minimum Pauli repulsion indicate shown around the C and N indicated by blue areas. The diagram with shaded surface and with projection effect of electron localization function (ELF) of NMA is also present in graph separately. The covalent bond regions of C-C and C-N have high LOL value, indicating high degree delocalization. The lowest degree of delocalization indicated by the blue regions in the molecule.

**Non-linear optical (NLO) property analysis:** The NLO properties of 1-methylnicotinamide (1-NMA) molecule in the gas phase at DFT/B3LYP/6-311++G(d,p) level was studied with the help of its polarizability, hyperpolarizability and dipole moment. Due to high sensitive of hyperpolarizabilities towards the B3LYP at 6-311++G (d,p) basis set applied [30-32]. The highest value of calculated dipole moment was in the X direction *i.e.* -6.43 D and dipole moments in the Y and Z directions were -2.57 and -2.00 D, respectively given in Table-3. Hence, there was strong interaction between the atoms, indicated by the high value of dipole moment (7.21 D) [33].

The reference value for NLO properties for molecular systems is taken of the urea molecule for comparison [34]. The total value of first order hyperpolarisability of given molecule calculated was  $2.05 \times 10^{-28}$  esu, which is higher than the urea ( $0.3728 \times 10^{-30}$  esu). This high value indicates considerable NLO properties. Thus this molecule may be used as a reference molecule for NLO analysis.

**Natural bond orbital (NBO) and natural hybrid orbital (NHO) analysis:** NBO analysis is one of the most important

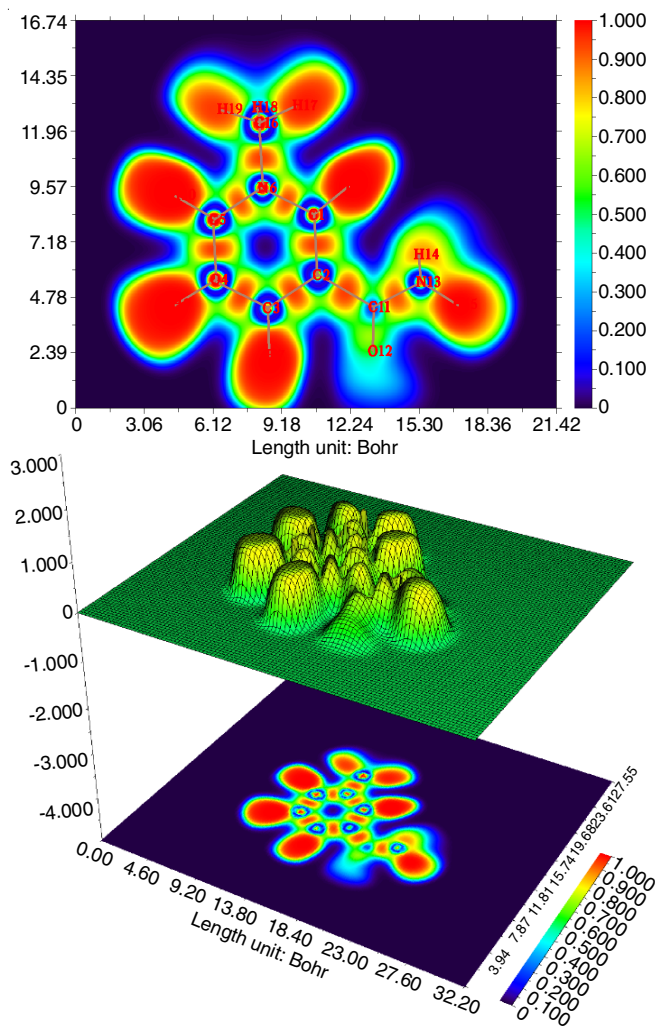


Fig. 5. Electron localization function (shaded surface map with projection effect and colour filled) of hydrogen bonding region in 1-methylnicotinamide (NMA)

TABLE-3  
THE VALUES OF CALCULATED DIPOLE MOMENT  $\mu(D)$ , POLARIZABILITY ( $\alpha_0$ ), FIRST ORDER HYPERPOLARIZABILITY ( $\beta_{tot}$ ) COMPONENTS OF 1-METHYLNICOTINAMIDE (1-NMA)

Parameters	B3LYP/6-311++G(d,p)	Parameters	B3LYP/6-311++G(d,p)
$\mu_x$	-6.4319	$\beta_{xxx}$	-47.4608
$\mu_y$	-2.5753	$\beta_{yxx}$	-37.9506
$\mu_z$	-1.9934	$\beta_{xyy}$	-8.0489
$\mu(D)$	7.2094	$\beta_{yyy}$	-1.5116
$\alpha_{xx}$	-33.3646	$\beta_{zxx}$	-13.8263
$\alpha_{xy}$	-6.0399	$\beta_{xzy}$	-5.9336
$\alpha_{yy}$	-37.9674	$\beta_{zyy}$	-8.2280
$\alpha_{xz}$	-6.4702	$\beta_{xzz}$	0.4377
$\alpha_{yz}$	-0.1056	$\beta_{yzz}$	-7.1410
$\alpha_{zz}$	-14.4183	$\beta_{zzz}$	1.4183
$\alpha_0$ (e.s.u)	$-4.23 \times 10^{-24}$	$\beta_{tot}$ (e.s.u)	$2.05 \times 10^{-28}$

study in the theoretical approach because it provides idea about the covalency effect, intra and intermolecular charge transfer (ICT), conjugation and hyperconjugation, *etc.* within the molecular system [35,36]. In order to evaluate the stabilizing energies of all the possible interaction between donor and acceptor

orbital, second order perturbation theory was used [37,38]. By using off diagonal elements of Fockmatrix in the NBO basis, the delocalization effect (or donor acceptor charge transfer) was estimated. For each donor (i) and acceptor (j), the stabilization energy (E2) associated with the delocalization of  $i \rightarrow j$  is determined by:

$$E^{(2)} = -n_{\sigma} \frac{(F_{ij})^2}{\epsilon_{\sigma^*} - \epsilon_{\sigma}}$$

where  $F_{ij}^2$  is the Fock matrix element between i and j NBO orbitals,  $\epsilon_{\sigma}$  and  $\epsilon_{\sigma^*}$  are the energies of bonding and antibonding NBO, respectively and  $n_{\sigma}$  the population of the donor s-orbital [39].

The donor-acceptor interactions in the form of perturbation energy given in Table-4. The  $\pi(C5-N6) \rightarrow \pi(C1-C2)$  and  $\pi^*(C3-C4)$  has 11.24 and 7.38 kJ/mol,  $\pi(C1-C2) \rightarrow \pi^*(C1-C2)$ ,  $\pi^*(C3-C4)$ ,  $\pi^*(C5-N6)$ ,  $\pi^*(C11-O12)$  and  $\pi^*(C11-N13)$  has 1.78, 19.72, 15.34, 10.67 and 0.67 kJ/mol and  $\pi(C3-C4)$

TABLE-4  
SECOND ORDER PERTURBATION THEORY OF THE FOCK MATRIX NBO ANALYSIS OF 1-METHYLNICOTINAMIDE (1-NMA)

Donor	Type	ED/e	Acceptor	Type	ED/e	E(2) (kcal/mol)	E(j)-E(i) (a.u.)	F(i,j) (a.u.)
C1-C2	$\sigma$	1.97690	C1-N6	$\sigma^*$	0.02755	1.72	1.19	0.040
			C1-H8	$\sigma^*$	0.01299	1.43	1.15	0.036
			C2-C3	$\sigma^*$	0.01938	3.27	1.30	0.058
			C2-C11	$\sigma^*$	0.08122	1.09	1.15	0.032
			C3-H7	$\sigma^*$	0.01294	1.97	1.21	0.044
			N6-C16	$\sigma^*$	0.01623	3.74	1.02	0.055
			C11-O12	$\sigma^*$	0.02950	1.02	1.36	0.033
C1-C2	$\pi$	1.62790	C1-C2	$\pi^*$	0.26459	1.78	0.29	0.021
			C3-C4	$\pi^*$	0.23275	19.72	0.31	0.072
			C5-N6	$\pi^*$	0.51197	15.34	0.22	0.054
			C11-O12	$\pi^*$	0.26093	10.67	0.37	0.058
			C11-N13	$\pi^*$	0.06603	0.67	0.77	0.022
C1-N6	$\sigma$	1.98472	C1-C2	$\sigma^*$	0.02065	1.81	1.43	0.045
			C2-C11	$\sigma^*$	0.08122	1.85	1.27	0.044
			C5-N6	$\sigma^*$	0.02680	2.56	1.32	0.052
			C5-H10	$\sigma^*$	0.01147	1.34	1.28	0.037
			N6-C16	$\sigma^*$	0.01623	1.10	1.15	0.032
C1-H8	$\sigma$	1.97961	C1-C2	$\sigma^*$	0.02065	1.35	1.12	0.035
			C2-C3	$\sigma^*$	0.01938	3.98	1.11	0.059
			C5-N6	$\sigma^*$	0.02680	5.45	1.01	0.066
C2-C3	$\sigma$	1.97444	C1-C2	$\sigma^*$	0.02065	3.18	1.27	0.057
			C1-H8	$\sigma^*$	0.01299	2.69	1.12	0.049
			C2-C11	$\sigma^*$	0.08122	1.47	1.12	0.037
			C3-C4	$\sigma^*$	0.01332	2.01	1.28	0.045
			C3-H7	$\sigma^*$	0.01294	0.82	1.18	0.028
			C4-H9	$\sigma^*$	0.01144	2.29	1.16	0.046
			C11-N13	$\sigma^*$	0.06603	1.36	1.20	0.037
C2-C11	$\sigma$	1.97194	C1-C2	$\sigma^*$	0.02065	1.78	1.19	0.041
			C1-N6	$\sigma^*$	0.02755	3.09	1.08	0.052
			C2-C3	$\sigma^*$	0.01938	1.59	1.19	0.039
			C3-C4	$\sigma^*$	0.01332	2.43	1.20	0.048
			C11-O12	$\sigma^*$	0.02950	0.82	1.25	0.029
			N13-H15	$\sigma^*$	0.00715	2.33	1.09	0.045
			C2-C3	$\sigma^*$	0.01938	2.26	1.27	0.048
C3-C4	$\sigma$	1.98052	C2-C11	$\sigma^*$	0.08122	2.66	1.13	0.050
			C3-H7	$\sigma^*$	0.01294	0.82	1.19	0.028
			C4-C5	$\sigma^*$	0.01361	2.14	1.28	0.047
			C4-H9	$\sigma^*$	0.01144	1.08	1.17	0.032
			C5-H10	$\sigma^*$	0.01147	2.36	1.13	0.046
			C1-C2	$\pi^*$	0.02065	16.99	0.27	0.064
			C5-N6	$\pi^*$	0.02680	46.60	0.20	0.088
C3-H7	$\sigma$	1.97743	C1-C2	$\sigma^*$	0.02065	4.49	1.08	0.062
			C2-C3	$\sigma^*$	0.01938	0.76	1.07	0.025
			C3-C4	$\sigma^*$	0.01332	0.64	1.09	0.024
			C4-C5	$\sigma^*$	0.01361	3.53	1.07	0.055
			C4-H9	$\sigma^*$	0.01144	0.61	0.97	0.022

C4-C5	$\sigma$	1.98048	C3-C4	$\sigma^*$	0.01332	2.22	1.31	0.048
			C3-H7	$\sigma^*$	0.01294	2.22	1.20	0.046
			C4-H9	$\sigma^*$	0.01144	0.77	1.19	0.027
			C5-N6	$\sigma^*$	0.02680	1.53	1.19	0.038
			C5-H10	$\sigma^*$	0.01147	1.14	1.15	0.032
C4-H9	$\sigma$	1.97687	N6-C16	$\sigma^*$	0.01623	3.96	1.02	0.057
			C2-C3	$\sigma^*$	0.01938	3.42	1.08	0.054
			C3-C4	$\sigma^*$	0.01332	0.83	1.09	0.027
			C4-C5	$\sigma^*$	0.01361	0.66	1.08	0.024
			C5-N6	$\sigma^*$	0.02680	4.83	0.98	0.061
C5-N6	$\sigma$	1.98550	C1-N6	$\sigma^*$	0.02755	2.63	1.32	0.053
			C1-H8	$\sigma^*$	0.01299	1.41	1.28	0.038
			C4-C5	$\sigma^*$	0.01361	1.35	1.43	0.039
			C4-H9	$\sigma^*$	0.01144	1.14	1.32	0.035
C5-N6	$\pi$	1.80998	N6-C16	$\sigma^*$	0.01623	1.13	1.15	0.032
			C1-C2	$\pi^*$	0.26459	19.38	0.39	0.079
			C3-C4	$\pi^*$	0.23275	7.38	0.40	0.049
C5-H10	$\sigma$	1.98093	C1-N6	$\sigma^*$	0.02755	5.58	1.00	0.067
			C3-C4	$\sigma^*$	0.01332	3.15	1.13	0.053
			C4-C5	$\sigma^*$	0.01361	1.04	1.11	0.030
C6-C16	$\sigma$	1.98632	C4-H9	$\sigma^*$	0.01144	0.55	1.01	0.021
			C1-C2	$\sigma^*$	0.02065	2.15	1.31	0.048
			C1-N6	$\sigma^*$	0.02755	1.32	1.20	0.036
			C1-H8	$\sigma^*$	0.01299	0.51	1.16	0.022
			C4-C5	$\sigma^*$	0.01361	2.04	1.31	0.046
C11-O12	$\sigma$	1.99364	C5-N6	$\sigma^*$	0.02680	1.30	1.20	0.035
			C5-H10	$\sigma^*$	0.01147	0.53	1.17	0.022
			C1-C2	$\sigma^*$	0.40857	1.40	1.55	0.042
			C2-C11	$\sigma^*$	0.02341	1.30	1.40	0.039
			C11-N13	$\sigma^*$	0.06603	1.50	1.48	0.043
C11-O12	$\sigma$	1.97712	N13-H14	$\sigma^*$	0.00905	0.76	1.44	0.030
			C1-C2	$\pi^*$	0.26459	4.08	0.38	0.038
			C11-O12	$\pi^*$	0.26093	0.77	0.46	0.018
C11-N13	$\sigma$	1.99343	N13-H14	$\pi^*$	0.00905	0.90	0.82	0.024
			C2-C3	$\sigma^*$	0.06603	1.24	1.37	0.037
			C11-O12	$\sigma^*$	0.02950	1.41	1.43	0.040
N13-H14	$\sigma$	1.98536	C11-O12	$\sigma^*$	0.26093	3.58	1.26	0.060
			C11-O12	$\sigma^*$	0.02950	2.04	0.73	0.037
N13-H15	$\sigma$	1.98822	C2-C11	$\sigma^*$	0.08122	4.28	1.03	0.060
			C11-O12	$\sigma^*$	0.02950	0.59	1.24	0.024
C16-H17	$\sigma$	1.98872	C5-N6	$\sigma^*$	0.02680	3.16	0.98	0.050
			C5-N6	$\sigma^*$	0.51197	0.62	0.47	0.018
C16-H18	$\sigma$	1.98200	C1-N6	$\sigma^*$	0.02755	0.67	0.97	0.023
			C5-N6	$\sigma^*$	0.51197	0.75	0.97	0.024
			C5-N6	$\sigma^*$	0.02680	2.39	0.46	0.034
C16-H19	$\sigma$	1.98875	C1-N6	$\sigma^*$	0.02755	3.26	0.97	0.050
			O12	LP(1)	1.97878	C2-C11	$\sigma^*$	0.08122
O12	LP(2)	1.84841	C11-N13	$\sigma^*$	0.06603	1.90	1.14	0.042
			C2-C11	$\pi^*$	0.08122	22.11	0.62	0.106
N13	LP(1)	1.73972	C11-N13	$\pi^*$	0.06603	24.29	0.70	0.119
			C11-O12	$\sigma^*$	0.02950	3.02	0.86	0.049
			C11-O12	$\pi^*$	0.26093	42.34	0.33	0.106

$\rightarrow\pi^*(C1-C2)$  and  $\pi^*(C5-N6)$  has 17.00 and 46.60 kJ/mol, which provide stabilization to the structure of studied molecule. Hyper conjugation between the *s*- and the *p*-electrons of C-C and C-N to the anti C-C and C-N bonds in the ring contributes in the stabilization of the ring, indicated in Table-5. The most stabilization energies are due to the three pairs of orbitals, namely (C5-N6), (C1-C2) and (C3-C4). The maximum occupancies

of (C11-O12) and (C11-N13) are 1.99364 and 1.99343, respectively. It confirms that  $\pi$ -character of hybrid orbitals are controlling these orbitals. For the acceptance of the Lewis structure of molecule the occupancies must be greater than 1.90, thus given occupancies are greater than this value therefore Lewis structure of 1-NMA is accepted. The interaction energy of resonance of title molecule were calculated by electron donating

TABLE-5  
HYBRID, POLARIZATION COEFFICIENT AND ATOMIC ORBITAL CONTRIBUTION IN  
SELECTED NATURAL BOND ORBITALS OF 1-METHYLNICOTINAMIDE (1-NMA)

Bond orbital	Hybrid A (h <sub>A</sub> )	Atomic orbital (%)	Polarization coefficient (c <sub>A</sub> )	Hybrid B (h <sub>B</sub> )	Atomic orbital (%)	Polarization coefficient (c <sub>B</sub> )
σ C1-C2	sp <sup>1.52</sup>	s(39.59%)p(60.37%)d(0.04%)	0.7066	sp <sup>1.92</sup>	s(34.28%)p(65.67%)d(0.05%)	0.7076
π C1-C2	sp <sup>1</sup>	s(0.01%)p(99.93%)d(0.06%)	0.7255	sp <sup>1</sup>	s(0.01%)p(99.95%)d(0.04%)	0.7255
σ C1-N6	sp <sup>2.45</sup>	s(28.99%)p(70.89%)d(0.12%)	0.6025	sp <sup>1.86</sup>	s(34.90%)p(65.05%)d(0.04%)	0.7981
σ C2-C3	sp <sup>1.89</sup>	s(34.57%)p(65.39%)d(0.04%)	0.7165	sp <sup>1.89</sup>	s(34.60%)p(65.36%)d(0.05%)	0.6976
σ C2-C11	sp <sup>2.21</sup>	s(31.14%)p(68.83%)d(0.04%)	0.7336	sp <sup>2</sup>	s(33.32%)p(66.63%)d(0.05%)	0.6796
σ C3-C4	sp <sup>1.84</sup>	s(35.22%)p(64.73%)d(0.05%)	0.7048	sp <sup>1.79</sup>	s(35.78%)p(64.18%)d(0.04%)	0.7094
π C3-C4	sp <sup>1</sup>	s(0.00%)p(99.91%)d(0.09%)	0.6709	sp <sup>1</sup>	s(0.00%)p(99.93%)d(0.07%)	0.7415
σ C4-C5	sp <sup>1.94</sup>	s(33.97%)p(65.98%)d(0.06%)	0.7023	sp <sup>1.54</sup>	s(39.41%)p(60.55%)d(0.04%)	0.7119
σ C5-N6	sp <sup>2.46</sup>	s(28.83%)p(71.05%)d(0.12%)	0.6006	sp <sup>1.86</sup>	s(34.98%)p(64.98%)d(0.04%)	0.7996
σ C5-N6	sp <sup>1</sup>	s(0.00%)p(99.83%)d(0.17%)	0.5428	sp <sup>1.83</sup>	s(0.01%)p(99.97%)d(0.02%)	0.8399
σ N6-C16	sp <sup>2.32</sup>	s(30.08%)p(69.90%)d(0.02%)	0.8137	sp <sup>3.48</sup>	s(22.30%)p(77.54%)d(0.16%)	0.5813
σ C11-O12	sp <sup>2.13</sup>	s(31.85%)p(67.98%)d(0.17%)	0.5979	sp <sup>1.62</sup>	s(38.07%)p(61.81%)d(0.13%)	0.8016
π C11-O12	sp <sup>1</sup>	s(1.69%)p(97.88%)d(0.43%)	0.5648	sp <sup>1</sup>	s(2.09%)p(97.78%)d(0.13%)	0.8252
σ C11-N13	sp <sup>2.04</sup>	s(32.85%)p(67.04%)d(0.10%)	0.6274	sp <sup>1.62</sup>	s(38.13%)p(61.81%)d(0.06%)	0.7787
LP(1)O12	sp <sup>0.67</sup>	s(59.90%)p(40.09%)d(0.02%)	—	—	—	—
LP(2)O12	sp <sup>1</sup>	s(0.01%)p(99.91%)d(0.08%)	—	—	—	—
LP(1)N13	sp <sup>24.90</sup>	s(3.86%)p(96.12%)d(0.02%)	—	—	—	—

from LP(1)N13→π\*(C11-O12) and σ\*(C11-O12) which have 42.34 and 3.02 kJ/mol and LP(2) O12→π\*(C2-C11) and π\*(C11-N13), which have stabilization energies 22.11 and 24.29 kJ/mol.

The information for the formation of complex is associated with the changes in NBO bond polarization and hybridization and the percentage changes of the studied compound 1-methylnicotinamide (1-NMA) given in Table-5. The σ (C1-C2) bond is built with sp<sup>1.52</sup> hybrid of carbon (possess 39.59% s, 60.37% p and 0.04% d-atomic orbitals) and sp<sup>1.92</sup> hybrid of carbon (34.28% s, 65.67% of p and 0.05% d-atomic orbitals). Thus NBO 1 showed bond of C1-C2 formed by overlapping of sp<sup>1.52</sup> hybrid of C1 and sp<sup>1.92</sup> hybrid of C2. Higher is the electronegativity then larger will be its polarization coefficient, C<sub>B</sub> (0.7076) for the C2 hybrid. This may be written as:

$$\sigma_{cc} = 0.7066(sp^{1.52})_{C1} + 0.7076(sp^{1.92})_{C2}$$

The polar (θ) and azimuthal (φ) angles of the vector for describing its p-component. The carbon NHO of the σC1-C2 and σC3-C4 bonds (NBO 1) are bent away C-C centers by 2.6 and 1.1 similarly σC1-N6 and σC5-N6 bonds are bent by 1.8 and 1.4, respectively. The prediction of change in direction of geometry is due to geometrical optimization and presented in Table-6.

**Population analysis:** The calculation of many properties like electronic structure, molecular polarizability, dipole moment and molecular reactivity depends upon atomic charges and the chemical shifts of atoms in NMR also depends on it. Mulliken population analysis (MPA) method with B3LYP functional was employed to calculate charges distribution on each the atoms of title molecule, tabulated in Table-7 and it's graph presented in Fig. 6. It is not a usual substituted pyridine ring because containing methyl group on ring nitrogen with positive charge. In the ring C1 and C4 are negative, while C2, C3, C5 and N6 are positive. There are five carbon atoms and one nitrogen atom in the ring, where amide group is attached at C2. C2 is more

TABLE-6  
NATURAL HYBRID ORBITAL DIRECTIONALITY AND  
BOND BENDING (DEVIATIONS FROM LINE OF NUCLEAR  
CENTERS) OF 1-METHYLNICOTINAMIDE (1-NMA)

Bond orbital	Deviation angle (°)		Line of centers	
	Hybrid A	Hybrid B	Polar (θ)	Azimuthal (φ)
σ C1-C2	2.6	2.6	94.3	43.7
π C1-C2	88.5	91.8	94.3	43.7
σ C1-N6	1.8	—	90.5	164.8
σ C2-C11	3.7	—	85.5	347.4
σ C3-C4	1.1	—	91.6	165.6
π C3-C4	90.4	90.2	91.6	165.6
σ C4-N5	1.6	2.5	85.7	226.1
σ C5-N6	1.4	—	84.5	285.7
π C5-N6	90.0	90.7	84.5	285.7
σ C11-O12	19.1	17.6	63.7	47.8
π C11-O12	80.3	79.1	63.7	47.8
σ C11-N13	2.3	1.5	110.0	287.8
π* C1-C2	88.5	91.8	94.3	43.7
π* C3-C4	90.4	90.2	91.6	165.6
π* C5-N6	90.0	90.7	84.5	285.7
π* C11-O12	80.3	79.1	63.7	47.8

positive than C3, C5 and nitrogen. Similarly, C1 is more negative than C4 in MPA. In routine, hydrogen atoms possess equal positive charges.

NBO charges used to calculate Fukui function values and tabulated in Table-7. Adding an electron in the molecule, in some spots shows by negative values of the Fukui function and *vice-versa*. Positive value of Δf(r) represent that atom is having nucleophilic attack and by negative value, having electrophilic attack. These values are given in Table-7. The reactivity order on the basis of calculated values of Fukui function for the electrophilic attack was C16 > N13 > C3 > C1 > C5 > C4. While for the nucleophilic attack the order is O12 > C2 > N6 > C11. On comparing all kind of attack like electrophilic, nucleophilic and radical attack it has been noted that electrophilic attack is greater than other two.

TABLE-7  
MULLIKEN CHARGE DISTRIBUTION, FUKUI FUNCTION AND LOCAL SOFTNESS CORRESPONDING TO (1,1), (2,2) AND (0,2) CHARGE AND MULTIPLICITY OF 1-METHYLNICOTINAMIDE (1-NMA)

Atom	Mulliken atomic charges			Fukui Functions				Local softness		
	N (+ 1, 1)	N-1 (+ 2, 2)	N + 1 (0, 2)	fr <sup>+</sup>	fr <sup>-</sup>	Δf(r)	fr <sup>0</sup>	sr <sup>+</sup> fr <sup>+</sup>	sr <sup>-</sup> fr <sup>-</sup>	sr <sup>0</sup> fr <sup>0</sup>
C1	-0.302598	-0.562979	-0.655093	-0.3525	0.260381	-0.61288	-0.04606	-0.08156	0.06025	-0.01066
C2	0.633412	0.706031	0.609315	-0.0241	-0.07262	0.048522	-0.04836	-0.00558	-0.0168	-0.01119
C3	0.336340	0.066119	-0.063150	-0.39949	0.270221	-0.66971	-0.06463	-0.09244	0.062527	-0.01496
C4	-0.003449	-0.210004	-0.295046	-0.2916	0.206555	-0.49815	-0.04252	-0.06747	0.047795	-0.00984
C5	0.140456	-0.061777	-0.208918	-0.34937	0.202233	-0.55161	-0.07357	-0.08084	0.046795	-0.01702
N6	0.206435	0.206474	0.233063	0.026628	-3.9E-05	0.026667	0.013295	0.006162	-9E-06	0.003076
C11	-0.344461	-0.342281	-0.339258	0.005203	-0.00218	0.007383	0.001512	0.001204	-0.0005	0.00035
O12	-0.251409	0.156995	-0.312022	-0.06061	-0.4084	0.347791	-0.23451	-0.01403	-0.0945	-0.05426
N13	0.239926	-0.249323	-0.370678	-0.6106	0.489249	-1.09985	-0.06068	-0.14129	0.113209	-0.01404
C16	0.345348	-0.280882	-0.291790	-0.63714	0.62623	-1.26337	-0.00545	-0.14743	0.144905	-0.00126

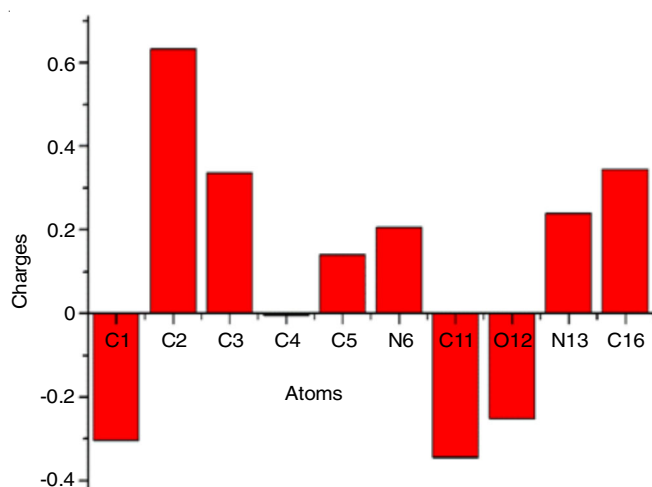


Fig. 6. The charges on the atoms of 1-methylnicotinamide (1-NMA) calculated by Mulliken population analysis (MPA) method

Fukui function is very useful to determine local softness which use to predict ligand-protein interactions, biological studies, proteins folding, *etc.* [40,41].

#### Frontier molecular orbital and UV-Vis spectral analysis:

The UV-visible spectra of the titled molecule in different solvent and gas phase was computed by DFT/PCM/B3LYP/6-311++G (d,p) approach. Fig. 7 shows plot of UV spectrum of 1-MNA, was computed in gas, methanol and DMSO solvent phases. Table-8 contained computed absorption wavelengths (energies) and other parameters. The calculated absorption wavelengths in gas phase are 356, 311 and 305 nm, whereas 290, 267 and 260 nm in DMSO solvent and similar absorption wavelengths are seen in methanol solvent. TD-DFT method utilized to calculate the electronic transitions. The slight variation in the absorption wavelength values in the gas phase and in solvent is due to the interaction between the positively charged 1-NMA molecule and polar solvents like DMSO and methanol. The values of wavelengths in gas phase and solvent phase clearly indicates that there is a influence of solvent on the optical activity of the molecule.

Molecular chemical stability is determined the energy by gap between HOMO and LUMO [42]. The energy gap between the HOMO → LUMO, HOMO-1 → LUMO+1, HOMO-2 → LUMO+2 and HOMO-3 → LUMO+3 were found 4.308, 5.468, 8.755 and 9.739 eV respectively, shown in Fig. 8. The energy gap also determines the electron transfer within the molecule,

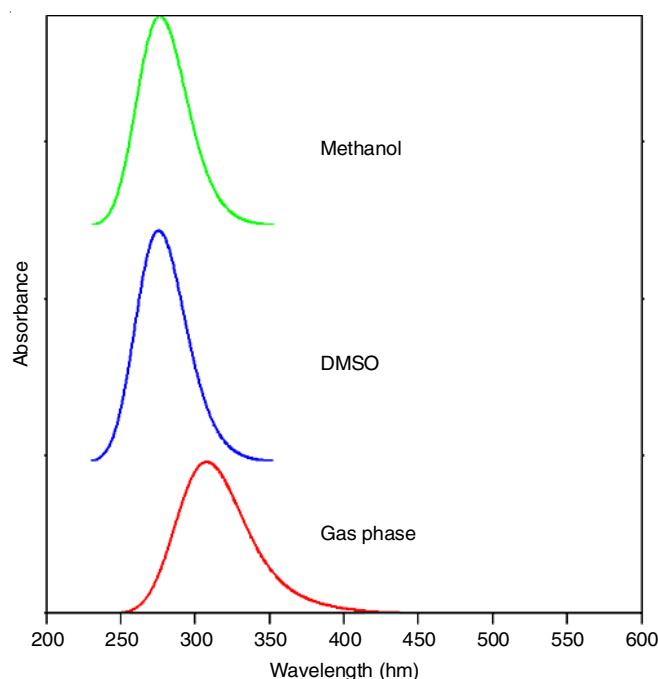


Fig. 7. UV-vis spectra of 1-methylnicotinamide (1-NMA), (theoretical- Gas phase, DMSO and methanol)

TABLE-8  
COMPARISON OF THE ELECTRONIC PROPERTIES OF 1-METHYLNICOTINAMIDE (1-NMA) IN GAS PHASE AND SOLVENT PHASE BY TD-DFT/B3LYP/6-311++G(d,p) METHOD

$\lambda_{cal}$ (nm)	Band gap (eV)	Energy (cm <sup>-1</sup> )	Oscillatory strength	Assignments
Gas phase				
356	3.4827	28089.7	0.0009	H→L(97%)
311	3.9832	32126.5	0.0038	H-1→L + 1(78%)
305	4.0634	32773.3	0.0081	H→L + 1(66%)
DMSO				
290	4.2814	34531.6	0.0007	H→L (92%)
267	4.6386	37408.6	0.0092	H-1→L(73%)
260	4.7654	38435.3	0.0092	H→L + 1(56%)
MeOH				
290	4.2740	34472	0.0006	H→L (92%)
267	4.6335	37371.5	0.0083	H-1→L(74%)
260	4.7609	38399	0.0084	H→L + 1(56%)

lower the energy gap higher in the electron conductivity and *vice-versa* [40].

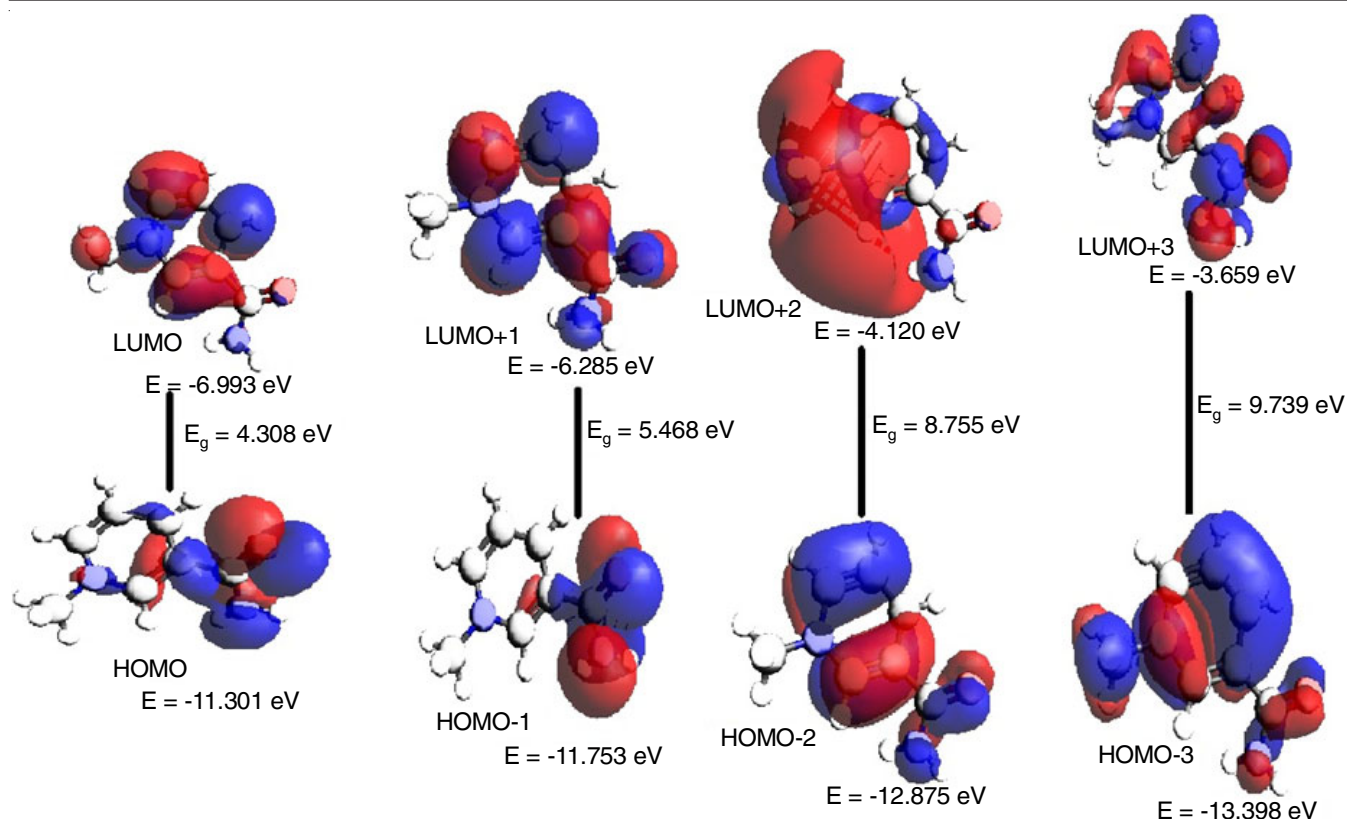


Fig. 8. Atomic orbitals HOMO, HOMO-1, HOMO-2, HOMO-3 and LUMO, LUMO+1, LUMO+2, LUMO+3 compositions of the frontier molecular orbital of 1-methylnicotinamide (1-NMA)

The chemical stability is also determined by the chemical hardness. The chemical hardness of the studied compound 1-NMA comes out to be 2.154, given in Table-9, higher the value of chemical hardness, the higher will be chemical stability of the compound. Similarly, calculated electronegativity was found 9.147. By using B3LYP method the electrophilicity index was 19.421. The moderate values were corresponding to a good agreement of energy transformation between the HOMO and LUMO [43].

TABLE-9 CALCULATED ENERGY VALUES OF 1-METHYLNICOTINAMIDE (1-NMA) BY B3LYP/6-311++G(d,p) METHOD	
Parameter	Values
$E_{\text{Homo}}$ (eV)	-11.301
$E_{\text{Lumo}}$ (eV)	-6.993
Ionization potential	11.301
Electron affinity	6.993
Energy gap (eV)	4.308
Electronegativity	9.147
Chemical potential	-9.147
Chemical hardness	2.154
Chemical softness	0.464
Electrophilicity index	19.421

Electrophilicity, hardness and chemical potential parameters are also predicted by DFT method, which was used in the prediction of many biological properties and for identification of reactive sites [44]. The conceptual density functional theory is also used to study bioactivities is the electrophilicity index [45], Electrophilicity index correlates with the toxico-

logical behaviour [46,47]. 1-NMA has an extremely low chemical softness 0. 0.464 indicating non-toxic behaviour of the studied molecule.

**Thermodynamical properties:** The thermodynamic properties of 1-NMA was also computed at different temperature using ORCA software, on the basis of vibrational analysis at B3LYP/6-311++G(d,p) level and the results had been detailed in Table-10. Enthalpy (H), Free energy (G), entropy (S) and these thermodynamic parameters of 1-NMA were calculated theoretically at different temperatures from 100 K to 500 K by using vibrational analysis. Since the vibrational intensities of the molecule increases with increase in temperature, therefore, rise in the temperature increases translational and rotational energies which in intern increase the thermodynamic quantities like enthalpy and entropy. This is well explained by the equipartition theorem [46,47]. The Gibb's free energy decreases with increasing temperature because it shows opposite property with H and S. To find the correlation between thermodynamic functions and temperatures, linear and quadratic formulas are

TABLE-10 TEMPERATURE DEPENDENCE OF PROPERTIES OF 1-METHYLNICOTINAMIDE (1-NMA) AT B3LYP/6-311++G(d,p)			
T(K)	$G_{\text{nm}}^0 \times 10$ (J/mol K)	$S_{\text{m}}^0$ (J/mol K)	$H_{\text{m}}^0$ (kJ/mol)
100	415.57	274.87	443.06
200	385.91	324.39	450.79
300	117.21	369.30	462.43
400	78.24	412.90	478.13
500	54.00	455.32	497.66

used as a correlation equation. For thermodynamic properties of the corresponding fitting factors ( $R^2$ ) were observed 1, 0.9454 and 1, respectively. The fitting equations are given as with correlation graph (Fig. 9).

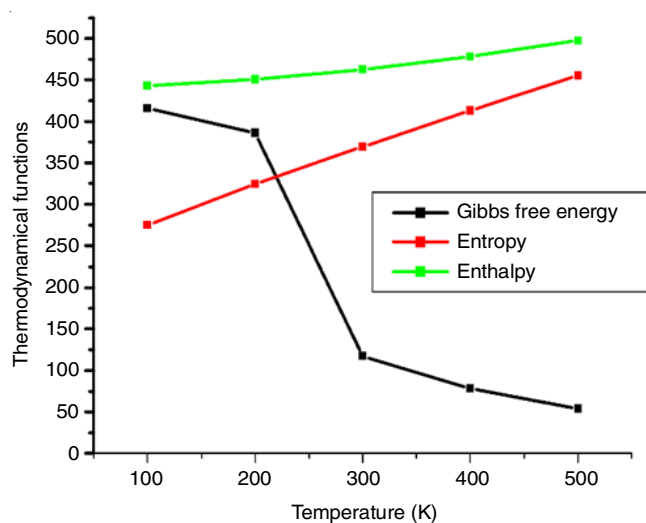


Fig. 9. Graphs representing dependence of entropy, Gibbs free enthalpy and enthalpy on temperature of 1-methylnicotinamide (1-NMA)

$$S = -0.0001T^2 + 0.5159T + 224.7780$$

$$G = 0.0017T^2 - 2.0618T + 639.7140$$

$$H = 0.0002T^2 + 0.0180T + 439.2820$$

**Molecular docking:** The target protein for docking was predicted using swiss ADME-Target prediction site. The docking has been done carefully by employing popular softwares like Chimera 1.14 [47] and Autodock vina [48]. The title molecule 1-NMA is docked with 4O8Z protein belongs to hydrolase domain. The best obtained binding energy found was -5.2 kcal/mol (Fig. 10) and all related values are present in Table-11. The bioactive nature of 1-MNA indicated by low value of binding energy. The hydrogen bond distance between bonded ligand and residue are found 1.922, 2.425, 2.374, 2.263 and 1.946 Å suggested the strong attachments of ligand with the taken

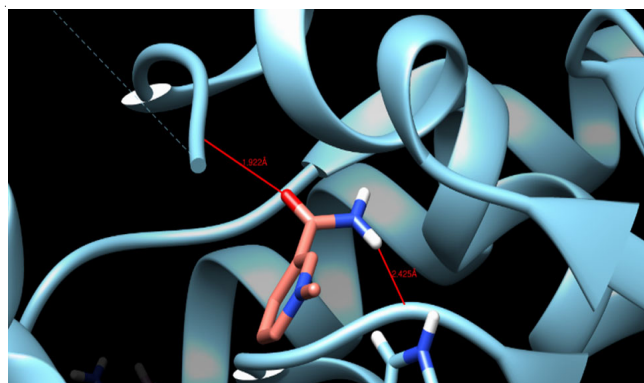


Fig. 10. Ligand 1-methylnicotinamide (1-NMA) embedded in the active site of 4O8Z protein

protein. The number of residue present in protein 4O8Z was 3 and the  $K_i$  value comes out to be 153.61.

**Drug-likeness:** For the fruitful growth in drug discovery and development, ligands structural properties are important factors. Druglikeness is used to interpret the balance between the molecular properties of the compound that influences its pharmacodynamics and pharmacokinetics and ultimately optimizes ADME. Different rules are involved for calculation like as Lipinski's rule, MDDR-like rule, Veber rule, Ghose filter, BBB rule, CMC-50 rule and QED [49]. 1-NMA has antithrombotic, anti-inflammatory, gastroprotective and vasoprotective properties.

The important ADME parameters such as hydrogen bond donors (HBD), hydrogen bond acceptors (HBA), molar refractivity (MR), Topological polar surface area (TPSA), Blood-brain barrier penetration (BBB), log  $k_p$  and bioavailability score for the known derivatives of 1-NMA was calculated and given in Table-12. The HBD and HBA should have values under 10, the calculated values for all tabulated compounds here are less than 3. The highest value of TPSA should be 140 Å<sup>2</sup>. The calculated values lies b 38 to 63 for all given molecules. In the same way, molar refractivity (MR value) must be somewhere in between 40 and 130 [50,51], the calculated MR value is < 40 which also for its derivatives.

TABLE-11  
HYDROGEN BONDING AND MOLECULAR DOCKING WITH  
CENTROMERE ASSOCIATED PROTEIN INHIBITOR PROTEIN TARGETS

Protein (PDB ID)	Number of residues	Inhibition constant ( $K_i$ ) (micromolar)	Bond distance (Å)	Binding energy (kcal/mol)	Reference RMSD (Å)
4O8Z	3	153.61	1.922, 2.425, 2.374, 2.263, 1.946	-5.20	8.63

TABLE-12  
ADME PROPERTIES OF 1-METHYLNICOTINAMIDE (1-NMA) AND RELATED COMPOUNDS

Derivatives	HBD	HBA	MR	TPSA Å <sup>2</sup>	GI absorption	BBB permeant	CYP1A2 inhibitor	log $k_p$ (cm/s)	Lipinski violations	Bioavail- ability score
1-Methylnicotinamide	1	1	<40	48.02	High	No	No	-10.25	0	0.55
4-Aminopyridine	1	1	<40	38.91	High	Yes	No	-6.65	0	0.55
4-Aminopyridine-2-carbonitrile	1	2	<40	62.70	High	No	No	-6.87	0	0.55
4-Aminonicotinaldehyde	1	2	<40	55.98	High	No	No	-6.92	0	0.55
2-Amino-4-fluoropyridine	1	2	<40	38.91	High	Yes	No	-6.56	0	0.55

HBD = Hydrogen bond donor, HBA = Hydrogen bond acceptor, MR = Molar refractivity, TPSA = Topological polar surface area, GI = Gastrointestinal, BBB = Blood-brain barrier penetration, log  $k_p$  = skin permeability.

GI absorption value is high as mentioned in Table-12, while BBB permeant is available for 4-aminopyridine and 2-amino-4-fluoropyridine only, skin permeability (log Kp) is between -6.56 to -10.25 and bioavailability score of 1-NMA and its derivative are same value of 0.55. By above said values for 1-NMA confirms its great importance and drug likeness.

## Conclusion

A thorough vibrational study of 1-methylnicotinamide (MNA) using B3LYP/6-311G++(d,p) method was carried out in this work. The calculated geometrical parameters were utilized as a base to investigate other properties. The theoretical simulations of IR and Raman spectra were also executed. There is a slight difference in values of absorption wavelength in gas and solvent phases, suggesting that there is an imperceptible effect on the optical activity of the molecule in the presence of solvent. The binding energies of the molecule were estimated by AIM analysis, the high energy of hydrogen bond indicating that they are actual covalent bonds. For studied molecule, the maximum stability of 42.34 KJ/mol is achieved by calculating resonance related interaction energy based on LP(1)N13→π\* (C11-O12) electron donating transition. The studied molecule can be represented as a new NLO organic moiety because of its higher estimated hyperpolarizability value compared to the urea which is taken as a reference NLO compound. From the HOMO-LUMO calculations, energy gap was found to be 4.308 eV, which suggests that the molecule is stable and also bioactive in nature. MEP visual depiction is used to identify reactive areas of the molecule and it is found that around N6, N13 and C16 atoms, the electrophilic character is maximum. The current investigation provides important information used as a starting point for the design of various bioactive amide containing molecules as a step prior to their synthesis and structural characterization. Molecular docking was also performed on the 4O8Z protein linked with the centromere showed a binding energy of -5.2 kcal/mol, thus providing its application in the medicinal field.

## ACKNOWLEDGEMENTS

The authors acknowledge the authorities of Dr. B.R. Ambedkar University, Agra, India for necessary infrastructure and facilities.

## REFERENCES

- J. Gebicki, A. Sysa-Jedrzejowska, J. Adamus, A. Wozniacka, M. Rybak and J. Zielonka, 1-Methylnicotinamide: A Potent Anti-inflammatory Agent of Vitamin Origin, *Pol. J. Pharmacol.*, **55**, 109 (2003).
- S. Chlopicki, J. Swies, A. Mogielnicki, W. Buczek, M. Bartus, M. Lomnicka, J. Adamus and J. Gebicki, 1-Methylnicotinamide (MNA), A Primary Metabolite of Nicotinamide, Exerts Anti-thrombotic Activity Mediated by a Cyclooxygenase-2/Prostacyclin Pathway, *Br. J. Pharmacol.*, **152**, 230 (2000); <https://doi.org/10.1038/sj.bjp.0707383>
- K. Bryniarski, R. Biedron, A. Jakubowski, J. Marcinkiewicz and S. Chlopicki, Anti-inflammatory Effect of 1-Methylnicotinamide in Contact Hypersensitivity to Oxazolone in Mice; Involvement of Prostacyclin, *Eur. J. Pharmacol.*, **578**, 332 (2008); <https://doi.org/10.1016/j.ejphar.2007.09.011>
- T.B. Domagala, A. Szeffler, L.W. Dobrucki, J. Dropinski, S. Polanski, M. Leszczynska-Wiloch, K. Kotula-Horowitz, J. Wojciechowski, L. Wojnowski, A. Szczeklik and L. Kalinowski, Nitric Oxide Production and Endothelium-Dependent Vasorelaxation Ameliorated by N<sup>1</sup>-Methylnicotinamide in Human Blood Vessels, *Hypertension*, **59**, 825 (2012); <https://doi.org/10.1161/HYPERTENSIONAHA.111.183210>
- K. Strom, D.M. Alamo, F. Ottosson, A. Edlund, L. Hjort, S.W. Jørgensen, P. Almgren, Y. Zhou, M. Martin-Rincon, C. Ekman, A. Pérez-López, O. Ekström, I. Perez-Suarez, M. Mattiasson, P. de Pablos-Velasco, N. Oskolkov, E. Ahlqvist, N. Wierup, L. Eliasson, A. Vaag, L. Groop, K.G. Stenkula, C. Fernandez, J.A.L. Calbet, H.-C. Holmberg and O. Hansson, N<sup>1</sup>-Methylnicotinamide is a Signalling Molecule Produced in Skeletal Muscle Coordinating Energy Metabolism, *Sci. Rep.*, **8**, 3016 (2018); <https://doi.org/10.1038/s41598-018-21099-1>
- M. Bartus, M. Fomnicka, R.B. Kostogrys, P. Kazmierczak, C. Watala, E.M. Slominska, R.T. Smoleński, P.M. Pisulewski, J. Adamus, J. Gębicki and S. Chlopicki, 1-Methylnicotinamide (MNA) Prevents Endothelial Dysfunction in Hypertriglyceridemic and Diabetic Rats, *Pharmacol. Rep.*, **60**, 127 (2008).
- A. Blazejczyk, M. Switalska, S. Chlopicki, A. Marcinek, J. Gebicki, M. Nowak, A. Nasulewicz-Goldeman and J. Wietrzyk, 1-Methylnicotinamide and its Structural Analog 1,4-dimethylpyridine for the Prevention of Cancer Metastasis, *J. Exp. Clin. Cancer Res.*, **35**, 110 (2016); <https://doi.org/10.1186/s13046-016-0389-9>
- J. Schmeisser, Mansfeld, D. Kuhlow, S. Weimer, S. Priebe, I. Heiland, M. Birringer, M. Groth, A. Segref, Y. Kanfi, N.L. Price, S. Schmeisser, S. Schuster, A.F.H. Pfeiffer, R. Guthke, M. Platzer, T. Hoppe, H.Y. Cohen, K. Zarse, D.A. Sinclair and M. Ristow, Role of Sirtuins in Lifespan Regulation is Linked to Methylation of Nicotinamide, *Nat. Chem. Biol.*, **9**, 693 (2013); <https://doi.org/10.1038/nchembio.1352>
- Menavitin Produkte, die das Molekül 1-MNA beinhalten: das Novel Food mit natürlicher Intelligenz, Startup Valley (in German) (2020).
- G.A. Petersson, A. Bennett, T.G. Tensfeldt, M.A. Al-Laham, W.A. Shirley and J. Mantzaris, A Complete Basis Set Model Chemistry. I. The Total Energies of Closed-shell Atoms and Hydrides of the First-Row Elements, *J. Chem. Phys.*, **89**, 2193 (1988); <https://doi.org/10.1063/1.455064>
- G.A. Petersson and M.A. Al-Laham, A Complete Basis Set Model Chemistry. II. Open-Shell Systems and the Total Energies of the First-Row Atoms, *J. Chem. Phys.*, **94**, 6081 (1991); <https://doi.org/10.1063/1.460447>
- M.J. Frisch, G.W. Trucks, H.B. Schlegel, G.E. Scuseria and M.A. Robb, R. Cheeseman, J. Montgomery, T. Vreven, K.N. Kudin, J.C. Burant, J.M. Millam, S.S. Iyengar, J. Tomasi, V. Barone, B. Mennucci, M. Cossi, G. Scalmani, N. Rega, G.A. Petersson, H. Nakatsuji, M. Hada, M. Ehara, K. Toyota, R. Fukuda, J. Hasegawa, M. Ishida, T. Nakajima, Y. Honda, O. Kitao, H. Nakai, M. Klene, X. Li, J.E. Knox, H.P. Hratchian, J.B. Cross, V. Bakken, C. Adamo, J. Jaramillo, R. Gomperts, R.E. Stratmann, O. Yazyev, A.J. Austin, R. Cammi, C. Pomelli, J.W. Ochterski, P.Y. Ayala, K. Morokuma, G.A. Voth, P. Salvador, J.J. Dannenberg, V.G. Zakrzewski, S. Dapprich, A.D. Daniels, M.C. Strain, O. Farkas, D.K. Malick, A.D. Rabuck, K. Raghavachari, J.B. Foresman, J.V. Ortiz, Q. Cui, A.G. Baboul, S. Clifford, J. Cioslowski, B.B. Stefanov, G. Liu, A. Liashenko, P. Piskorz, I. Komaromi, R.L. Martin, D.J. Fox, T. Keith, M.A. Al-Laham, C.Y. Peng, A. Nanayakkara, M. Challacombe, P.M.W. Gill, B. Johnson, W. Chen, M.W. Wong, C. Gonzalez, J.A. Pople, Gaussian 03, Revision C. 02, Gaussian Inc., Wallingford, CT (2004).
- F. Neese, The ORCA Program System, *WIREs Comput. Mol. Sci.*, **2**, 73 (2012); <https://doi.org/10.1002/wcms.81>
- M.H. Jomroz, Vibrational Energy Distribution Analysis, VEDA4, Warsaw (2004).
- A. Daina, O. Michielin and V. Zoete, SwissADME: A Free Web Tool to Evaluate Pharmacokinetics, Drug-likeness and Medicinal Chemistry Friendliness of Small Molecules, *Sci. Rep.*, **7**, 42717 (2017); <https://doi.org/10.1038/srep42717>
- T. Lu and F. Chen, Multiwfn: A Multifunctional Wavefunction Analyzer, *J. Comput. Chem.*, **33**, 580 (2012); <https://doi.org/10.1002/jcc.22885>
- Origin 8.0, OriginLab Corp., Northampton, MA (2007).
- C.S. Abraham, J.C. Prasana, S. Muthu, F. Rizwana B and M. Raja, Quantum Computational Studies, Spectroscopic (FT-IR, FT-Raman and UV-Vis) Profiling, Natural Hybrid Orbital and Molecular Docking

- Analysis on 2,4-Dibromoaniline, *J. Mol. Struct.*, **1160**, 393 (2018); <https://doi.org/10.1016/j.molstruc.2018.02.022>
19. G. Socrates, *Infrared and Raman Characteristic Group Frequencies, Table and Charts*, Wiley: Chichester, Ed. 3 (2001).
  20. L.J. Bellamy, *The Infrared Spectra of Complex Molecules*, Chapman and Hall: London, vol. 2 (1980).
  21. M. Tsuboi, <sup>15</sup>N Isotope Effects on the Vibrational Frequencies of Aniline and Assignments of the Frequencies of its nh<sub>2</sub> Group, *Spectrochim. Acta*, **16A**, 505 (1960); [https://doi.org/10.1016/0371-1951\(60\)80046-X](https://doi.org/10.1016/0371-1951(60)80046-X)
  22. G. Varsanyi, *Assignments for Vibrational Spectra of Seven Hundred Benzene Derivatives*, Academia Kiado: Budapest, vols. 1 and 2 (1973).
  23. G. Varsanyi, *Vibrational Spectra of Seven Hundred Benzene Derivatives*, Academic Press: New York (1969).
  24. L.J. Bellamy, *The Infrared Spectra of Complex Molecules*, John Wiley: New York (1959).
  25. A.J. Barnes, M.A. Majid, M.A. Stuckey, P. Gregory and C.V. Stead, The Resonance Raman Spectra of Orange II and Para Red: Molecular Structure and Vibrational Assignment, *Spectrochim. Acta A Mol. Biomol. Spectrosc.*, **41**, 629 (1985); [https://doi.org/10.1016/0584-8539\(85\)80050-7](https://doi.org/10.1016/0584-8539(85)80050-7)
  26. S. Pinchas, D. Samuel and M. Weiss-Brodav, The Infrared Absorption of <sup>18</sup>O-labelled Benzamide, *J. Chem. Soc.*, 1688 (1961); <https://doi.org/10.1039/jr9610001688>
  27. J.S. Murry and K. Sen, *Molecular Electrostatic Potential Concepts and Applications*, Elsevier: Amsterdam (1996).
  28. O. Haji-Ghassemi, R.J. Blackler, N.M. Young and S.V. Evans, Antibody Recognition of Carbohydrate Epitopes, *Glycobiology*, **25**, 920 (2015); <https://doi.org/10.1093/glycob/cwv037>
  29. J. Poater, M. Duran, M. Solà and B. Silvi, Theoretical Evaluation of Electron Delocalization in Aromatic Molecules by Means of Atoms in Molecules (AIM) and Electron Localization Function (ELF) Topological Approaches, *Chem. Rev.*, **105**, 3911 (2005); <https://doi.org/10.1021/cr030085x>
  30. H. Sekino and R.J. Bartlett, Hyperpolarizabilities of the Hydrogen Fluoride Molecule: A Discrepancy Between Theory and Experiment?, *J. Chem. Phys.*, **84**, 2726 (1986); <https://doi.org/10.1063/1.450348>
  31. J. Henriksson, T. Saue and P. Norman, Quadratic Response Functions in the Relativistic Four-component Kohn-Sham Approximation, *J. Chem. Phys.*, **128**, 024105 (2008); <https://doi.org/10.1063/1.2816709>
  32. J.P. Hermann, D. Ricard and J. Ducuing, Optical Nonlinearities in Conjugated Systems:  $\beta$ -Carotene, *Appl. Phys. Lett.*, **23**, 178 (1973); <https://doi.org/10.1063/1.1654850>
  33. S. Debrus, H. Ratajczak, J. Venturini, N. Pincon, J. Baran, J. Barycki, T. Glowiak and A. Pietraszko, Novel Nonlinear Optical Crystals of Noncentrosymmetric Structure Based on Hydrogen Bonds Interactions Between Organic and Inorganic Molecules, *Synth. Met.*, **127**, 99 (2002); [https://doi.org/10.1016/S0379-6779\(01\)00607-5](https://doi.org/10.1016/S0379-6779(01)00607-5)
  34. C. Cassidy, J.M. Halbout, W. Donaldson and C.L. Tang, Nonlinear Optical Properties of Urea, *Opt. Commun.*, **29**, 243 (1979); [https://doi.org/10.1016/0030-4018\(79\)90027-0](https://doi.org/10.1016/0030-4018(79)90027-0)
  35. C.S. Abraham, J.C. Prasana and S. Muthu, Quantum Mechanical, Spectroscopic and Docking Studies of 2-Amino-3-bromo-5-nitropyridine by Density Functional Method, *Spectrochim. Acta A Mol. Biomol. Spectrosc.*, **181**, 153 (2017); <https://doi.org/10.1016/j.saa.2017.03.045>
  36. F. Weinhold and L.C. Randis, *Valency and Bonding: A Natural Bond Orbital Donor-Acceptor Perspective*, Cambridge University Press (2005).
  37. C. James, A.A. Raj, R. Reghunathan, V.S. Jayakumar and I.H. Joe, Structural Conformation and Vibrational Spectroscopic Studies of 2,6-bis(*p*-N,N-Dimethyl benzylidene)cyclohexanone using Density Functional Theory, *J. Raman Spectrosc.*, **37**, 1381 (2006); <https://doi.org/10.1002/jrs.1554>
  38. J. Liu, Z. Chen and S. Yuan, Study on the Prediction of Visible Absorption Maxima of Azobenzene Compounds, *J. Zhejiang Univ. Sci.*, **6**, 584 (2005); <https://doi.org/10.1631/jzus.2005.B0584>
  39. G. Varsanyi, *Vibrational Spectra of Benzene Derivatives*, Academic Press: New York, NY, USA (1969).
  40. K. Fukui, Role of Frontier Orbitals in Chemical Reactions, *Science*, **218**, 747 (1982); <https://doi.org/10.1126/science.218.4574.747>
  41. S. Balachandar and M. Dhandapani, Biological Action of Molecular Adduct Pyrazole:Trichloroacetic Acid on *Candida albicans* and ctDNA - A Combined Experimental, Fukui Functions Calculation and Molecular Docking Analysis, *J. Mol. Struct.*, **1184**, 129 (2019); <https://doi.org/10.1016/j.molstruc.2019.02.006>
  42. N.M. O'boyle, A.L. Tenderholt and K.M. Langner, cclib: A Library for Package-Independent Computational Chemistry Algorithms, *J. Comput. Inside Chem.*, **29**, 839 (2008); <https://doi.org/10.1002/jcc.20823>
  43. S. Xavier and S. Periandy, Spectroscopic (FT-IR, FT-Raman, UV and NMR) Investigation on 1-Phenyl-2-nitropropene by Quantum Computational Calculations, *Spectrochim. Acta A Mol. Biomol. Spectrosc.*, **149**, 216 (2015); <https://doi.org/10.1016/j.saa.2015.04.055>
  44. A. Shalini, H. Tandon and T. Chakraborty, Molecular Electrophilicity Index - A Promising Descriptor for Predicting Toxicological Property, *J. Bioequiv. Bioavailab.*, **9**, 528 (2017); <https://doi.org/10.4172/jbb.1000356>
  45. R. Parthasarathi, V. Subramanian, D.R. Roy and P.K. Chattaraj, Electrophilicity Index as a Possible Descriptor of Biological Activity, *Bioorg. Med. Chem.*, **12**, 5533 (2004); <https://doi.org/10.1016/j.bmc.2004.08.013>
  46. D.R. Roy, R. Parthasarathi, B. Maiti, V. Subramanian and P.K. Chattaraj, Electrophilicity as a Possible Descriptor for Toxicity Prediction, *Bioorg. Med. Chem.*, **13**, 3405 (2005); <https://doi.org/10.1016/j.bmc.2005.03.011>
  47. E.F. Pettersen, T.D. Goddard, C.C. Huang, G.S. Couch, D.M. Greenblatt, E.C. Meng and T.E. Ferrin, UCSF Chimera-A Visualization System for Exploratory Research and Analysis, *J. Comput. Chem.*, **25**, 1605 (2004); <https://doi.org/10.1002/jcc.20084>
  48. G.M. Morris, R. Huey, W. Lindstrom, M.F. Sanner, R.K. Belew, D.S. Goodsell and A.J. Olson, AutoDock4 and AutoDockTools4: Automated Docking with Selective Receptor Flexibility, *J. Comput. Chem.*, **30**, 2785 (2009); <https://doi.org/10.1002/jcc.21256>
  49. A. Daina, O. Michielin and V. Zoete, iLOGP: A Simple, Robust, and Efficient Description of *n*-Octanol/Water Partition Coefficient for Drug Design using the GB/SA Approach, *J. Chem. Inf. Model.*, **54**, 3284 (2014); <https://doi.org/10.1021/ci500467k>
  50. C.A. Lipinski, F. Lombardo, B.W. Dominy and P.J. Feeney, Experimental and Computational Approaches to Estimate Solubility and Permeability in Drug Discovery and Development Settings, *Adv. Drug Deliv. Rev.*, **23**, 3 (1997); [https://doi.org/10.1016/S0169-409X\(96\)00423-1](https://doi.org/10.1016/S0169-409X(96)00423-1)
  51. S. Aayisha, T.S. Renuga Devi, S. Janani, S. Muthu, M. Raja and S. Sevvanthi, DFT, Molecular Docking and Experimental FT-IR, FT-Raman, NMR Inquisitions on 4-Chloro-N-(4,5-dihydro-1H-imidazol-2-yl)-6-methoxy-2-methylpyrimidin-5-amine: Alpha-2-imidazoline Receptor Agonist Antihypertensive Agent, *J. Mol. Struct.*, **1186**, 468 (2019); <https://doi.org/10.1016/j.molstruc.2019.03.056>